Archives of Biochemistry and Biophysics 633 (2017) 68–77

Contents lists available at ScienceDirect

Archives of Biochemistry and Biophysics

journal homepage: www.elsevier.com/locate/yabbi

Non-thermal plasma induces mitochondria-mediated apoptotic signaling pathway *via* ROS generation in HeLa cells

Wei Li [a, g, *], K.N. Yu [c], Jie Ma [b, d], Jie Shen [e], Cheng Cheng [e], Fangjian Zhou [a], Zhiming Cai [g], Wei Han [b, f, **]

[a] Department of Urology, Sun Yat-Sen University Cancer Centre, Guangzhou 510060, China
[b] Center of Medical Physics and Technology, Hefei Institutes of Physical Sciences, Chinese Academy of Sciences, Anhui Province, China
[c] Department of Physics, City University of Hong Kong, Tat Chee Avenue, Kowloon Tong, Hong Kong
[d] University of Science and Technology of China, Hefei, Anhui, China
[e] Institute of Plasma Physics, Hefei Institutes of Physical Sciences, Chinese Academy of Sciences, Anhui Province, China
[f] Collaborative Innovation Center of Radiation Medicine of Jiangsu Higher Education Institutions and School for Radiological and Interdisciplinary Sciences (RAD-X), Soochow University, Suzhou, Jiangsu, China
[g] Shenzhen Second People's Hospital, The First Affiliated Hospital of Shenzhen University, Shenzhen 518036, China

ARTICLE INFO

Article history:
Received 27 July 2017
Received in revised form
4 September 2017
Accepted 7 September 2017
Available online 9 September 2017

Keywords:
Non-thermal plasma
Reactive oxygen species
HeLa cell
Apoptosis
Mitochondria

ABSTRACT

Non-thermal plasma (NTP) has been proposed as a novel therapeutic method for anticancer treatment. Although increasing evidence suggests that NTP selectively induces apoptosis in some types of tumor cells, the molecular mechanisms underlying this phenomenon remain unclear. In this study, we further investigated possible molecular mechanisms for NTP-induced apoptosis of HeLa cells. The results showed that NTP exposure significantly inhibited the growth and viability of HeLa cells. Morphological observation and flow cytometry analysis demonstrated that NTP exposure induced HeLa cell apoptosis. NTP exposure also activated caspase-9 and caspase-3, which subsequently cleaved poly (ADP- ribose) polymerase. Furthermore, NTP exposure suppressed Bcl-2 expression, enhanced Bax expression and translocation to mitochondria, activated mitochondria-mediated apoptotic pathway, followed by the release of cytochrome *c*. Further studies showed that NTP treatment led to ROS generation, whereas blockade of ROS generation by N-acetyl-L-cysteine (NAC, ROS scavengers) significantly prevented NTP-induced mitochondrial alteration and subsequent apoptosis of HeLa cells *via* suppressing Bax translocation, cytochrome *c* and caspase-3 activation. Taken together, our results indicated that NTP exposure induced mitochondria-mediated intrinsic apoptosis of HeLa cells was activated by ROS generation. These findings provide insights to the therapeutic potential and clinical research of NTP as a novel tool in cervical cancer treatment.

1. Introduction

Non thermal plasma (NTP), known as the fourth state of matter, is generated by ionization of neutral gas molecules [1,2]. Due to advances in physics and biotechnology, NTP has been widely used for various biomedical applications, such as blood coagulation, wound healing, and tissue and device sterilization [3–5]. In addition, newly developed NTP exert anti-tumor effects in various cancer cell types both *in vitro* and *in vivo*, including skin, pancreatic, and head and neck cancers [6–8]. Further studies showed that these effects were primarily due to the formation of reactive oxygen species (ROS including H_2O_2, OH^-, O_2^-, O_3) [9]. Previous studies have demonstrated that Amon these species, O_2^- and H_2O_2 can penetrate to a depth that is sufficient to reach cells, where iron proteins could conceivably catalyze both radicals into a highly reactive OH radical that interact with cellular components [10]. Although basal levels of ROS serve as a physiological regulator of cell functions, excessive ROS can lead to damages of biological

Abbreviations: NTP, Non-thermal plasma; ROS, reactive oxygen species; NAC, N-acetyl-L-cysteine; $\Delta\psi m$, Mitochondrial transmembrane potential; PARP, poly ADP-ribose polymerase; Z-VAD-FMK, pan caspase inhibitor; PI, Propidium Iodine; Bcl-2, B-Cell CLL/Lymphoma 2; Bax, BCL2 associated X protein; DCFDA, 2,7- dichlorofluorescein diacetate; O_2^-, superoxide anion; H_2O_2, hydrogen peroxide.

* Corresponding author. 350 Shushanghu Road, 230031 Hefei, Anhui, China.
** Corresponding author. 350 Shushanghu Road, 230031 Hefei, Anhui, China.
E-mail addresses: qwer_214@163.com (W. Li), hanw@hfcas.ac.cn (W. Han).

http://dx.doi.org/10.1016/j.abb.2017.09.005
0003-9861/

molecules such as DNA strand breaks and protein modification, resulting in cell damage and apoptosis [11].

Apoptosis or programmed cell death is an important and well-controlled physiological process that occurs during embryonic development and tissue remodeling through eliminating unneeded or damaged cells with potentially harmful mutations [12]. It is well known that there are two main signaling pathways to control apoptosis, namely, the death-receptor-mediated extrinsic pathway and mitochondria-mediated intrinsic pathway [13,14]. The former pathway is initiated mainly by binding of death receptors to their ligands (e.g. Fas and its ligand FasL) to activate caspase-8 [15]. The mitochondria-mediated intrinsic pathway is associated with the release of cytochrome *c* from mitochondria into the cytoplasm, where it binds to the adaptor molecule apoptotic protease activating factor-1 (Apaf-1) and subsequently activating caspase-9 [14]. Previous studies demonstrated that ROS played a crucial role in the mitochondria apoptotic pathway. ROS accumulation was able to enhance apoptosis by collapsing the mitochondrial potential, inducing mitochondrial oxidation channel, and releasing cytochrome *c* from mitochondria to the cytosol [16,17]. In addition, Bcl-2 family proteins played a key role in regulating cell death and survival mainly by regulating the permeability of the mitochondria [18]. According to their function, Bcl-2 family proteins have traditionally been classified into two kinds, anti-apoptosis proteins (e.g., Bcl-2) and pro-apoptosis proteins (e.g., Bax) [18].

Our previous studies showed that low-dose NTP exposure inhibited the invasiveness of the human cervical cancer HeLa cells, but high-dose exposure significantly inhibited the cell viability. However, the molecular mechanisms for this phenomenon are still unknown. In this study, our results indicated that NTP exposure triggered HeLa cell apoptosis *via* inducing ROS accumulation and mitochondrial membrane potential loss.

2. Materials and methods

2.1. Cell culture and reagents

HeLa cells, which were used in our previous studies, were cultured in DMEM medium (Gibco, Carlsbad, CA, USA) with 10% fetal calf serum (Thermo Scientific Hyclone, Logan, UT, USA), 100 U/mL of penicillin and 100 μg/mL of streptomycin (Gibco, Carlsbad, CA, USA). All cultures were maintained in a 37 °C, 5% CO_2 humidified atmosphere.

The primary antibodies for Caspase-3(CST, 9662), PARP (CST, 9542), Bax (CST, 2774), Bcl-2 (CST, 2872), Caspase-9 (CST, 9502), cytochrome *c* (CST, 4272), Cox IV (CST, 11967) and β −actin (CST, 4970) were purchased from Cell Signaling Technology Inc. (Beverly, MA, USA). Horseradish peroxidase (HRP)-conjugated secondary antibody was purchased from Santa Cruz Biotechnology (Santa Cruz, CA, USA). BCA Protein Assay Kit and enhanced chemiluminescence (ECL) reagents were purchased from Pierce (Rockford, IL, USA). CCK-8, trypan blue, Annexin V-FITC/Propidium Iodine (PI) apoptosis detection kit, JC-1 Mitochondrial Potential Detection Kit, DCFH-DA, RIPA lysis buffer and phenylmethyl sulfonylfluoride (PMSF) were purchased from Beyotime Inst. Biotech (Beijing, China). Caspases colorimetric assay kits were purchased from (Keygen Biotech, China). Polyvinylidene difluouride (PVDF) membrane were purchased from Millipore Corp (Bedford, MA, USA). Pan-caspase inhibitor was purchased from Selleck Chemicals (Houston, TX, USA). NAC and Hoechst 33324 were purchased from Sigma Chemical Inc. (St. Louis, MO, USA). All other chemicals and reagents were of the highest quality and obtained from standard commercial sources.

2.2. DBD plasma device

The atmospheric pressure DBD plasma was developed in our laboratory as previously described [9]. Briefly, four DBD plasma reactors were sealed in a hollow plexiglass cylinder as a reactor chamber with two air inlet and outlet holes. The high-voltage electrode was a copper cylinder with a diameter of 32 mm covered by a quartz glass with a thickness of 1 mm as an insulating dielectric barrier. The ground electrode was a copper cylinder with a diameter of 37 mm. The discharge gap between the bottom of the quartz and the treated sample surface was 5 mm. The alternating current power supply was a commercial transformer capable of continuous and tunable output voltages and frequencies. The applied voltage and discharge current of the DBD plasma were monitored with a Tektronix MSO 5104 digital oscilloscope. Helium gas entered the chamber from the gas inlet (flow rate was 80 L/h). Helium was injected into the chamber 5 min before the experiment to expel air originally inside the chamber. NTP was generated at a voltage of 12 kV and a frequency of 24 kHz (discharge power density was about 0.9 W/cm^2).

2.3. Cell culture and plasma treatment

For NTP exposure, 3×10^5 cells were plated onto 30 mm diameter Petri dishes with 2 ml DMEM culture medium. After 12 h incubation, the medium was replaced with 2 ml fresh culture medium. The distance between the nozzle and the surface of DMEM was fixed at 10 mm. Then cells were exposed to NTP for 60 or 80 s, incubated for a further 24 h and then harvested for the next experiments. The control cells (NTP exposure for 0 s) were subjected to identical procedures except the plasma treatment. A gas-only treatment (helium) was used to confirm the presence or absence of effects from the gas alone.

2.4. Cell death assay

The living cell population was analyzed using Trypan Blue dye exclusion assay. After 24 or 48 h incubation, both floating and trypsinized adherent cells were collected. Mixture of cell suspension and 0.4% trypan blue (v:v = 1:1) was loaded onto a haemocytometer (Neubauer Improved, Marienfeld, Germany) for counting under a light microscope.

Cell viability was determined with the CCK8. Briefly, cell suspensions (3×10^3 cells/ml) were seeded in a 96-multiwell plate. After 12 h incubation, cells were exposed to plasma for 60 or 80 s for 24 h, and CCK8 solution (10 μl) was then added to each well for 2 h at 37 °C. The absorbance (A) and optical density (OD) of each well was then determined using a microplate reader (Multiskan MK3, USA) at 455 nm of wavelength.

2.5. Nucleus morphology of apoptotic cells

HeLa cells were exposed to plasma for 60 or 80 s. After 24 h incubation, the cells were washed with PBS for three times, and stained with Hoechst 33324 (15 μg/mL) for 10 min in dark. The fluorescent images of HeLa cell nuclei were captured with a phase-contrast fluorescent microscope (Leica DMI 40008, Germany).

2.6. Flow cytometry analysis of apoptosis

Annexin V-FITC/Propidium Iodine (PI) apoptosis detection kit (Beyotime Inst. Biotech, Beijing, China) was used for apoptosis detection. Briefly, cells were collected and washed twice with PBS, and then re-suspended with 500 μl 1 × Annexin V binding buffer (containing 5 μl of Annexin V-FITC and 5 μl of PI). After 10 min

incubation in dark at room temperature, the cells were analyzed by flow cytometry (Accuri C6, BD Biosciences, Bedford, MA, USA).

2.7. Observation of H_2O_2 and ROS production

The level of H_2O_2 was analyzed by a commercial Kit (Beyotime Institute of Biotechnology, China) and measured the absorbance at 560 nm using amicroplate reader (Bio-TEK, USA). In this kit, ferrous ions (Fe^{2+}) were oxidative to ferric ions (Fe^{3+}) by H_2O_2. The Fe^{3+} then forms a complex with an indicator dye xylenol orange causing an increase in absorbance at 560–590 nm measurable as a purple colored complex.

ROS were detected with the cell-permeable fluorescent-probe 2′-7′-dichlorofluorescein diacetate (DCFH-DA) (Beyotime Inst. Biotech, Beijing, China). For ROS imaging, the cells were stained with 10 μM DCFH-DA at 37 °C for 30 min in dark and then washed with PBS for three times, and subsequently the fluorescent images were captured with a fluorescence microscope (Leica DMI 40008, Germany).

For ROS quantification, cells were collected and incubated with 10 μM DCFH-DA at 37 °C for 30 min in the dark. Then cells were washed twice with PBS and were analyzed with flow cytometer.

2.8. Mitochondrial transmembrane potential ($\Delta\psi m$) detection

The JC-1 Mitochondrial Potential Detection Kit (Beyotime Inst. Biotech, Beijing, China) was used to measure the mitochondrial depolarization of HeLa cells. For imaging, the cells were stained with JC-1 solution for 15 min at room temperature in the dark, and then the fluorescent images were captured with a fluorescence microscope (Leica DMI 40008, Germany).

For quantification of $\Delta\psi m$ rates, the cells were collected and incubated with JC-1 staining solution for 30 min in the dark. The cells were then washed twice with PBS and were analyzed with flow cytometer.

2.9. Detection of caspase activity

The activities of caspase-3, 8 and 9 were measured with *Caspases colorimetric assay kits* (KeyGen Biotech Co., Ltd., Nanjing, China) according to the manufacturer's recommendations. After incubation, the cells were trypsinized and harvested by centrifugation. Cell lysis buffer was added to the cell pellets and protein concentrations were measured using BCA Protein Assay Reagent (Pierce, Rockford, IL, US). Afterwards, 150 μg of each cell lysate was incubated with each caspase substrate at 37 °C in a microplate for 4 h. After incubation, the samples were read with a microplate spectrophotometer (ELx800, BioTek Instruments Inc., USA) at 405 nm.

2.10. RNA extraction and real-time quantitative PCR assays

Total RNA was extracted from cells using TRIZOL Reagent (Invitrogen, USA), and cDNA was synthesized from 1 μg of RNA with the M-MLV Reverse Transcriptase Kit (Promega, USA) as recommended by the manufacturer.

Real-time quantitative PCR reactions for the quantification of gene expression were performed with Bio-Rad iQ5 Real Time PCR System. The primers sequence was: TGCTTCAGGGTTTCATCCAG (forward); AACATTTCAGCCGCCACTC (reverse) for Bax; TTCGCCG AGATGTCCAGTCAGC (forward); GTTGACGCTCTCCACACACA (reverse) for Bcl-2. The primers of β-actin were synthesized as described [19]. Relative abundances of the target mRNAs were calculated as described.

2.11. Western blot analysis

Total protein was extracted as described previously. In addition, isolation of mitochondrial and cytosolic proteins was performed using the Mitochondria/cytosol Fractionation Kit (Pierce, Rockford, IL, US). Protein concentration was determined with the BCA Protein Assay Kit (Pierce, Rockford, IL, USA). Equivalent amounts of proteins samples were uploaded and separated by 12% SDS-PAGE and then electro-transferred to polyvinylidene difluouride (PVDF) membranes (Millipore Corp, Atlanta, GA, US). The membranes were blocked in 5% non-fat dry milk powder at room temperature for 1 h, and then incubated with primary antibodies for overnight at 4 °C, followed by HRP-conjugated secondary antibodies at room temperature for 1 h. The signals of bands were detected by ECL reagents.

2.12. Statistical analysis

All experiments were performed in triplicates, and the results were expressed as the mean ± SD. Statistical significance was determined using the Student's *t*-test. A *p*-value smaller than 0.05 was considered to correspond to a statistically significant difference.

3. Results

3.1. NTP exposure inhibits HeLa cell growth via induction of cell apoptosis

Previous studies showed that NTP exposure significantly lowered the viability of HeLa cells [19]. In our study, the cell viability was assessed using the cell growth curve and Trypan blue exclusion assays. The results showed that NTP exposures for 60 or 80 s significantly inhibited cell growth (Fig. 1A) and promoted the cell death (Fig. 1B) in a dose-dependent manner at 24 or 48 h after the NTP exposures.

To determine whether apoptosis was involved in NTP-induced cell death, we studied the morphological changes of the cells using phase-contrast microscopy. Microscopic observations revealed that the HeLa cells began to shrink and retracted from their neighbors after NTP exposure of 60 s when compared with the control. With NTP exposure increased to 80 s, most of the HeLa cells became rounded and shriveled, while some cells burst or became floating (Fig. 2A, upper panel). We also examined the chromatin condensation after NTP exposures by Hoechst 33342 staining. The results (Fig. 2A, bottom panel) showed that typical apoptotic morphologies, characterized by condensed chromatin and nuclear fragmentation (white arrow), appeared after NTP exposures of 60 and 80 s when compared with the control cells, the latter exhibiting round nuclei with well distributed chromatin. Furthermore, the results in Fig. 2B showed that the percentage of apoptotic cells (early-phase and late-phase apoptotic cells) significantly increased from 8.5% of the control to 28.0% (NTP exposure of 60 s) and 37.7% (NTP exposure of 80 s) (Fig. 2B). Taken together, these results indicated that NTP exposures induced HeLa cells apoptosis in a dose-dependent manner.

3.2. NTP exposure induced apoptosis is mediated by activation of caspases in HeLa cells

To investigate the mechanisms of apoptosis induced by NTP exposures, we detected the activities of several vital caspases (including caspase-8, -9 and -3). The results shown in Fig. 3A revealed that the activity of caspase-8 did not change when compared to the control group, but caspase-9 and -3 increased

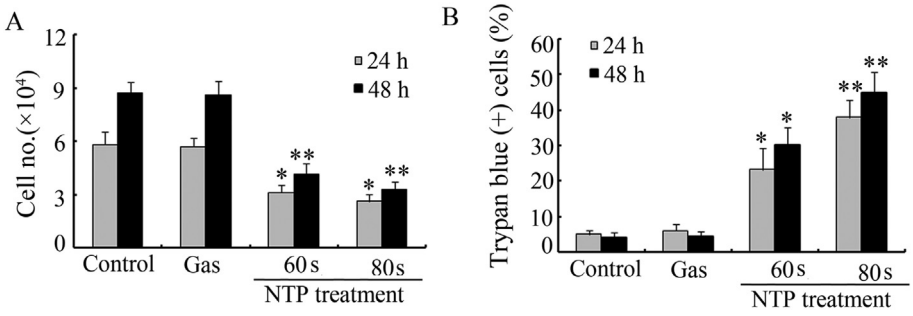

Fig. 1. NTP exposure induced growth inhibition and death of HeLa cells. HeLa cells were exposed to NTP for 60 or 80 s. (A) Growth inhibition was assessed using the trypan blue exclusion test dye exclusion assay. (B) Dead cells were determined as: trypan blue (+) cells ratio (%) = (stained cell number/total cell number) × 100. Data are expressed as means ± SD for three independent experiments with triplicates. $^{*}p < 0.05$; $^{**}p < 0.01$ versus control (NTP exposure time for 0 s).

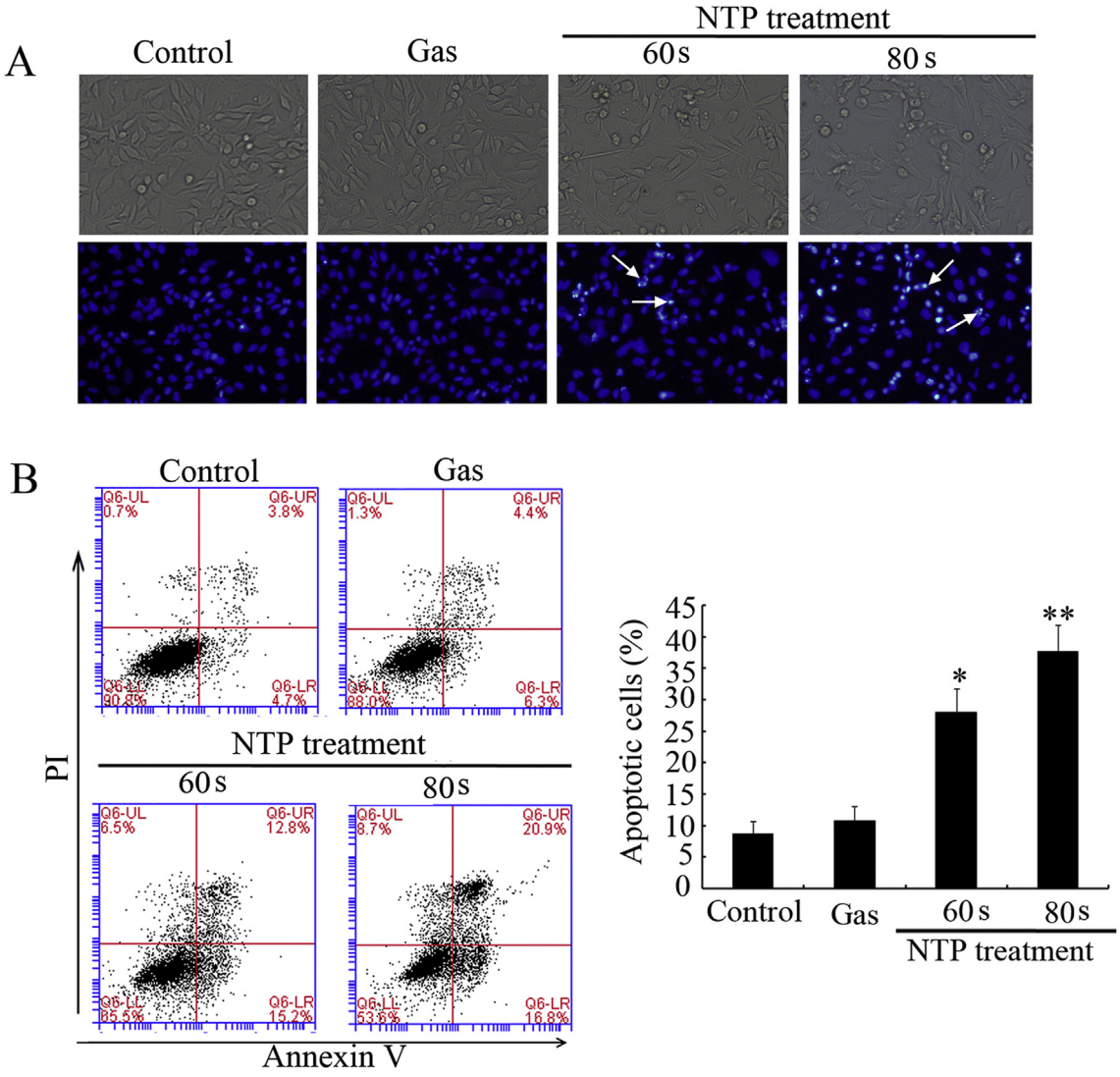

Fig. 2. NTP exposure induced HeLa cell apoptosis. (A) Cell morphological changes were assessed using phase-contrast microscope (upper panel). Nuclear morphological changes were observed under fluorescent microscope after Hoechst 33342 staining, and white arrows indicated cells exhibiting chromatin condensation (bottom panel). (B) Flow cytometry analysis of NTP induced apoptosis. The Annexin V-staining cells represent total apoptosis cells. The results are mean ± SD and mean values of three independent experiments. $^{*}p < 0.05$; $^{**}p < 0.01$ versus control (NTP exposure time for 0 s).

significantly in a dose-dependent manner after NTP exposures of 60 or 80 s. The results of western blot (Fig. 3B) also showed that full-length procaspase-3 decreased with increased NTP dose, and the cleaved form increased accordingly. The cleavage of Poly (ADP-ribose) polymerase (PARP), a well-known substrate for caspase-3 cleavage during apoptosis, was also observed after NTP exposures of 60 or 80 s (Fig. 3B).

In order to study whether activation of caspase cascade was

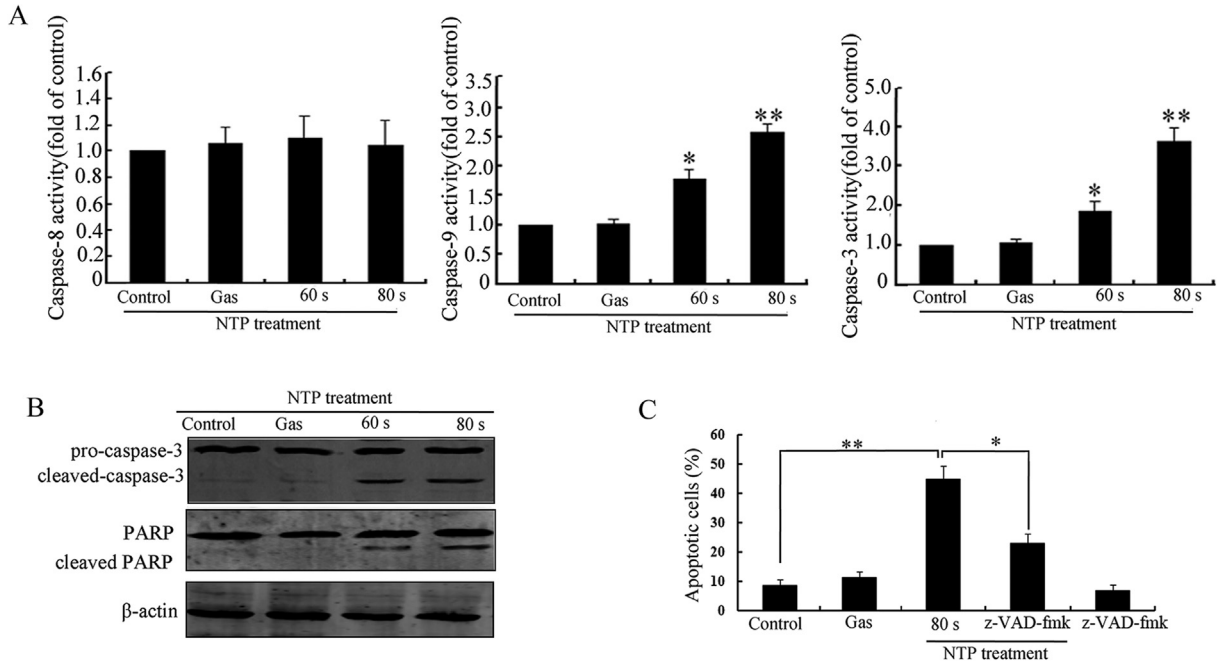

Fig. 3. NTP exposure induced HeLa cell apoptosis depends on caspase activation. **(A)** The activities of caspase-3, -8 and -9 were determined using Caspase activity kit. Data were expressed as means ± SD from three independent experiments with triplicates in each experiment. (B) Western blot analysis of caspase-3 and PARP proteins in NTP-treated HeLa cells. Images are representative of three independent experiments. (C) Effect of pan-caspase inhibitor on NTP-induced apoptosis. Cells were incubated with 20 μM of pan-caspase inhibitors for 2 h and then exposed to NTP for 80s. After 24 h incubation, the effects of pan-caspase inhibitors (20 μM) on NTP-induced apoptosis were studied through flow cytometry. The data shown are representative of three independent experiments. $^{*}p < 0.05$; $^{**}p < 0.01$ versus control (NTP exposure time for 0 s).

necessary for NTP-induced apoptosis, pan-caspase inhibitor (z-VAD-fmk) was used to inhibit the intracellular protease, and NTP-induced apoptosis was then analyzed using flow cytometry. The results in Fig. 3C showed that z-VAD-fmk significantly decreased the apoptotic rate of cells exposed to NTP. These results suggested that NTP-induced apoptosis was dependent on caspase activation in HeLa cells.

3.3. NTP exposure induced apoptosis is associated with ROS generation

Our group have previously demonstrated that H_2O_2 produced by NTP were the predominant species for induction of cell death [20]. So H_2O_2 concentration was determined by a commercial kit. The results (Fig. 4A) showed that after NTP exposure for 60 and 80 s, there was a significantly increase in the H_2O_2 content of HeLa cells compared with control group (nearly 3.8- and 5.1-fold, respectively). In addition, H_2O_2 and O_2^- can be catalyzed into a highly reactive OH radical by iron proteins, so total ROS generation was detected with DCFH-DA. The results (Fig. 4B C) showed that NTP exposure induced distinct increase ROS levels.

The contribution of ROS to apoptosis was further assessed by pretreating the HeLa cells with the ROS scavenger N-acetyl-L-cysteine (NAC). The viability (assessed with CCK8) of cells pretreated with NAC and then exposed to NTP (80 s) increased significantly when compared to those without NAC pretreatment (Fig. 5A), while the apoptotic percentage of cells showed an opposite trend (Fig. 5B). These results suggested that the generation of ROS induced by NTP exposure mediated the apoptosis.

3.4. NTP exposure reduces mitochondrial membrane potential

To further explore the effect of NTP on the mitochondrial membrane potential (Δψm), we used JC-1 as the fluorescence probe to evaluate changes in Δψm by fluorescence microscopy and flow cytometry. Typical images shown in Fig. 6A revealed more green fluorescence in NTP-exposed cells than the controls, which suggested that NTP exposure induced depolarization of the mitochondria membrane. Further flow cytometry analyses demonstrated that the Δψm−depolarized cells increased distinctly from 6.3% of the control to 24.1% and 41.3% after exposure to NTP for 60 and 80 s, respectively (Fig. 6B). In addition, pretreatment with NAC decreased the ratio of Δψm−depolarized cells after NTP exposure (Fig. 6B). All these results indicated that NTP treatment reduced the mitochondrial membrane potential through the production of ROS.

3.5. NTP exposure activates mitochondrial apoptotic pathway

It is established that the mitochondrial membrane potential (Δψm) is determined by the balance of pro-apoptotic and anti-apoptotic Bcl-2 family members, such as Bax and Bcl-2 [16]. Bcl-2 protects cells from apoptosis induction by interacting with Bax to maintain Δψm and block the release of pro-apoptotic proteins. Therefore, Real-time RT-PCR and western blot were used to explore the effects of NTP exposure on Bcl-2 and Bax expression. The results (Fig. 7A B) showed that NTP exposure significantly increased Bax expression in a dose-dependent manner at both mRNA and protein levels. On the contrary, the expression of Bcl-2 was significantly decreased in a dose-dependent manner at both mRNA and protein levels (Fig. 7A B). Accordingly, the ratio of Bax/Bcl-2 in NTP-exposed cells increased compared with the control group, which favored the induction of apoptosis (Fig. 7C).

Previous studies demonstrated that Bax could translocate to the mitochondria from cytosol, then activated the permeability transition pores and thereby allowed the release of cytochrome *c* to the cytosol [12]. In the present study, mitochondria and cytosol fractions were isolated separately and analyzed by western blot. The results (Fig. 7D) showed that NTP exposure promoted the translocation of Bax from cytosol to mitochondria. Consistent with this

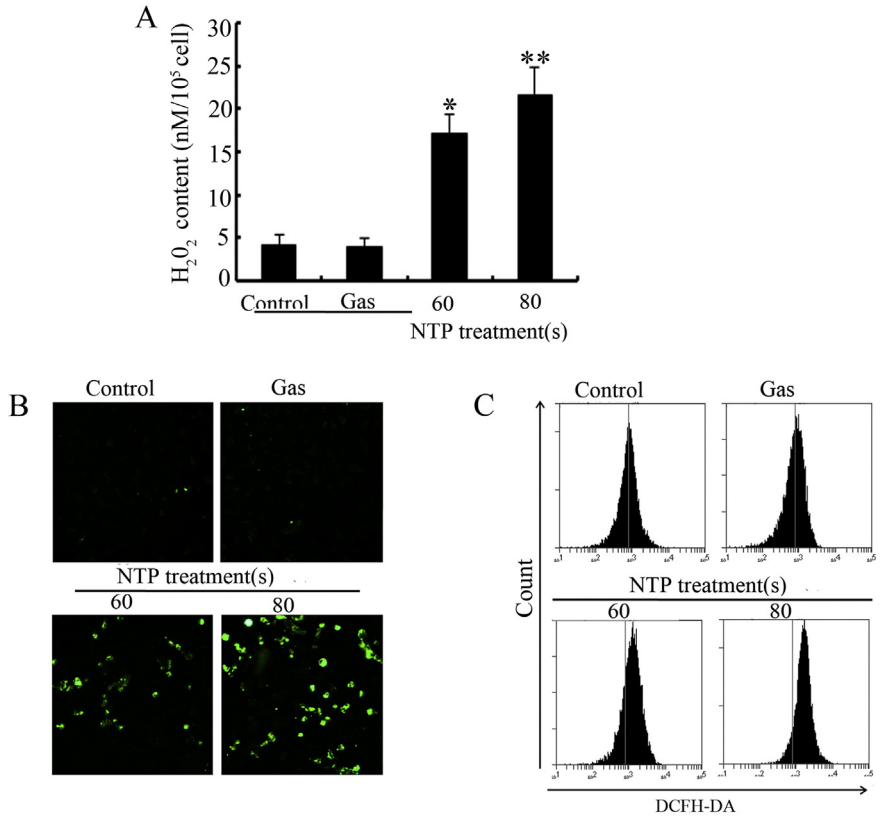

Fig. 4. NTP exposure leads to H_2O_2 and ROS generation in HeLa cells. (A) HeLa cells were exposed to plasma for 60 or 80 s. After 24 h incubation, the intracellular H_2O_2 levels was analyzed by a commercial Kit. (B) HeLa cells were stained with DCFH-DA and ROS generation was observed under fluorescence microscope (C) The levels of ROS after NTP exposure were analyzed by flow cytometry. The data are shown as mean ± SD of three independent experiments.
$^*p < 0.05$; $^{**}p < 0.01$ versus control (NTP exposure time for 0 s).

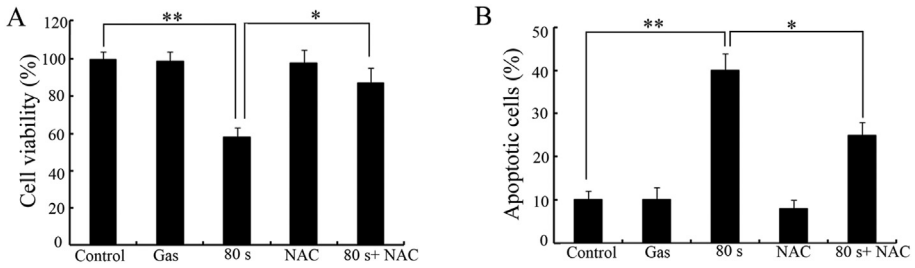

Fig. 5. The role of ROS in NTP-induced apoptosis. The cells were or were not pretreated with ROS inhibitors (NAC, 5 mM) for 2 h, and then exposed to NTP for 80s. (A) After 24 h incubation, cell viability was assessed using CCK8 assay. (B) The effect of ROS scavengers on the apoptotic percentage of NTP-induced cells. The apoptotic percentage was determined using flow cytometry. The data are shown as mean ± SD of three independent experiments.
$^*p < 0.05$; $^{**}p < 0.01$ versus control (NTP exposure time for 0 s).

observation, the presence of cytochrome *c* in the cytosolic fraction from NTP-exposed cells were also noted (Fig. 7D), while cytochrome *c* was only detected in the mitochondria fraction in the controls (Fig. 7D). These results suggested that NTP exposure induced apoptosis through activation of the mitochondrial pathway.

In addition, to further explore the roles of ROS in NTP induced apoptosis, we investigated the effects of NAC on the expression of Bcl-2, Bax and the redistribution of cytochrome *c*. The results (Fig. 8A B) showed that NAC pretreatment effectively attenuated the expression of Bcl-2, the translocation of Bax from cytoplasm to mitochondria, and the release of mitochondrial cytochrome *c* to cytoplasm induced by NTP exposure. These results suggested that ROS played a critical role in activation of mitochondrial apoptosis induced by NTP exposure.

4. Discussion

NTP has been proposed as a novel therapeutic method for anticancer treatments [6,21,22]. Although increasing evidence suggests that NTP induces apoptosis in various cancer cell types, the underlining signal pathways is still unknown. In the present study, we provided evidence that NTP inhibited the growth of HeLa cells *via* induction of apoptosis, which was activated by ROS generation and mitochondria-mediated apoptotic signaling pathways.

NTP has recently been applied to living cells and tissues, and has emerged as a novel tool for biomedical applications (e.g., wound healing, blood coagulation and cancer treatment) [3,5,23]. Among these, a low dose of NTP was reported to be able to stimulate endothelial cell growth to accelerate wound healing *via* releasing fibroblast growth factor-2 or facilitate blood coagulation *via*

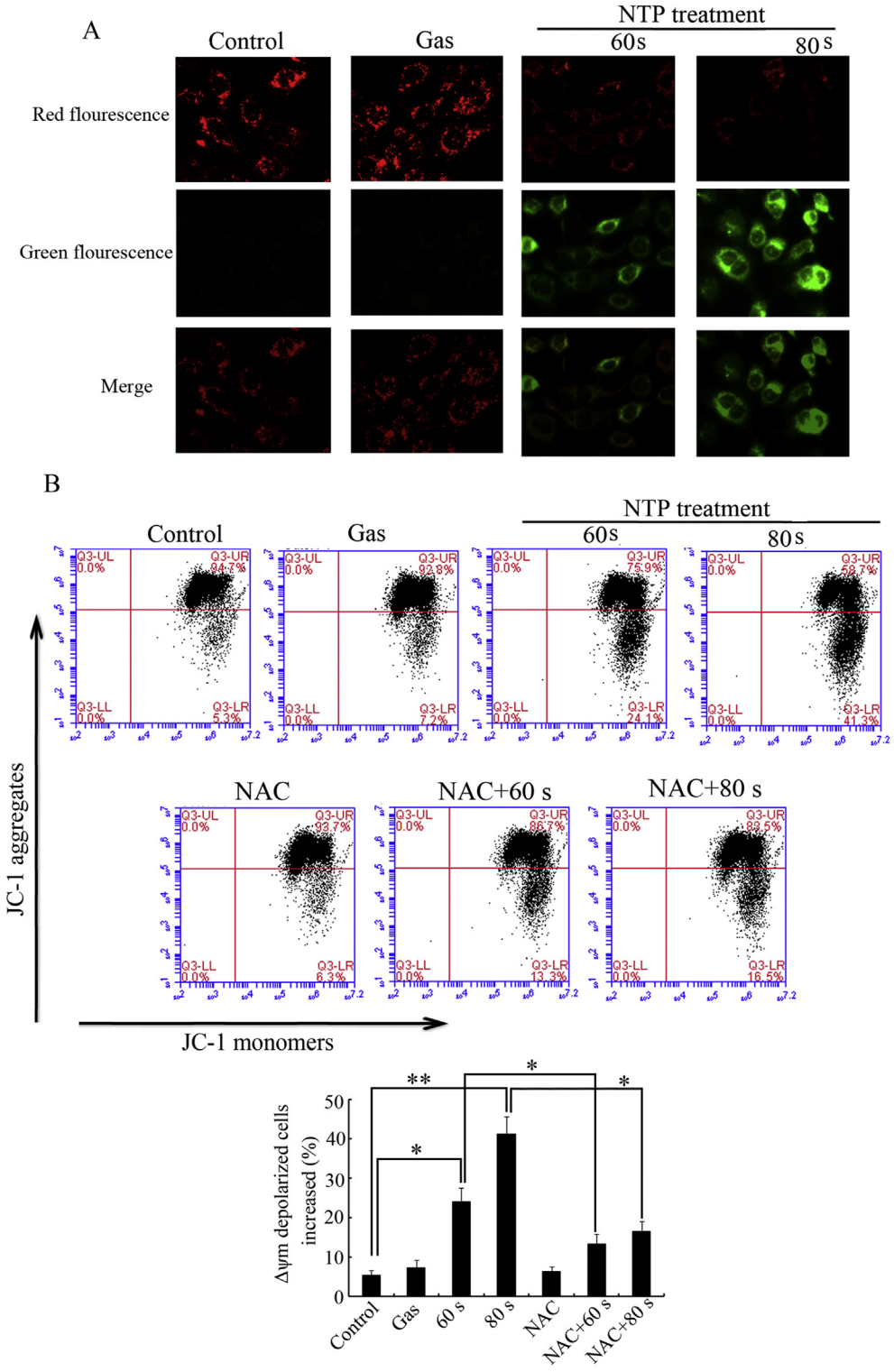

Fig. 6. NTP exposure reduced mitochondrial membrane potential in HeLa cells. HeLa cells were exposed to NTP for 60 or 80s, and then stained with JC-1 for 15 min at room temperature. (A) Mitochondrial membrane potential (Δψm) was assessed using fluorescent microscope. Red fluorescence represents the mitochondrial aggregation form of JC-1 indicating intact mitochondrial membrane potential. Green fluorescence represents the monomeric form of JC-1 indicating a dissipation of Δψm. (B) The Δψm was analyzed by flow cytometry. The data are shown as mean ± SD of three independent experiments. $^{*}p < 0.05$; $^{**}p < 0.01$ versus control (NTP exposure time for 0 s).

promoting layer formation and protein cross-linking on the blood sample surface [4,5]. In contrast, a high dose preferentially leads to cytotoxic effects on tumor cells (such as senescence, apoptosis or necrosis) *via* different mechanisms [6,21,22]. In addition, combining NTP with cetuximab can decrease invasiveness in cetuximab-resistant oral squamous cancer cells through inhibition of the NF-κB pathway [24]. Our previous studies also found that low dose NTP (exposures for 20 and 40 s) could restrain the

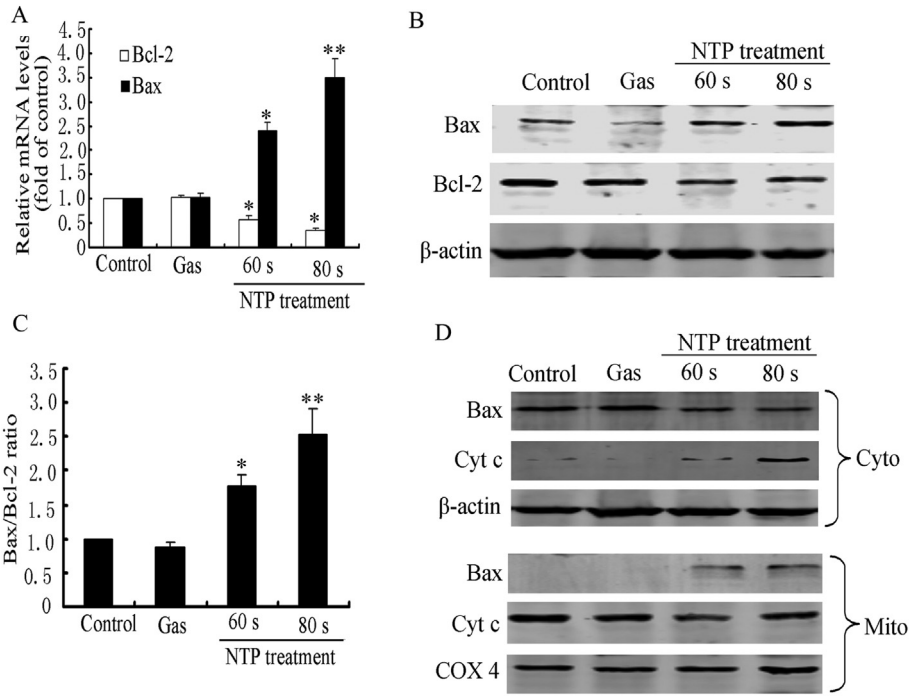

Fig. 7. NTP-induced apoptosis of HeLa cells was mediated by activation of mitochondrial pathway. (A) Bax and Bcl-2 mRNA levels were determined by Real time RT-PCR using β-actin (housekeeping gene) as an internal control. (B) Expression of Bax and Bcl-2 were determined by western blot. (C) Effect of NTP exposure on the ratio of Bax/Bcl-2. (D) Localization of Bax and cytochrome *c* in subcellular fraction of HeLa cells. Mitochondrial and cytosolic proteins were isolated and analyzed by western blot. COX 4 and β-actin were used as internal controls for the mitochondrial fraction and the cytosolic fraction, respectively. All the data shown are from three independent experiments. $^{*}p < 0.05$; $^{**}p < 0.01$ versus control (NTP exposure time for 0 s).

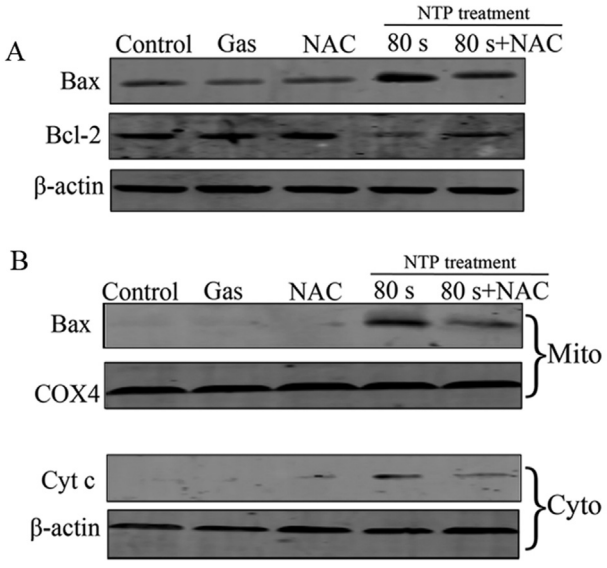

Fig. 8. Role of ROS in NTP-reduced mitochondrial membrane potential. The cells were or were not pretreated with ROS inhibitors (NAC, 5 mM) for 2 h, and then exposed to NTP for 80s. (A) The expression of Bcl-2 and Bax were determined by western blot. (B) The localization of Bax and cytochrome *c* were isolated and analyzed by western blot. COX 4 and β-actin were used as internal controls for the mitochondrial fraction and the cytosolic fraction, respectively. All the data shown are from three independent experiments.

invasiveness of HeLa cells by suppressing the MAPK pathway and decreasing MMP-9 expression [19]. In the present study, we further showed that high-dose NTP exposures (for 60 and 80 s) significantly suppressed growth and promoted death of HeLa cells. Important features of apoptotic cell death (including cellular shrinkage, chromatin condensation and phosphatidylserine externalization) were observed after NTP exposures. These results indicated that NTP inhibited the growth of HeLa cells through induction of apoptosis instead of necrosis.

Apoptosis plays an important role in the treatment of cancer [25,26]. Apoptosis includes at least two main processes, namely, the death receptor pathway and the mitochondrial pathway [27]. Caspase-8 and -9 are initiator caspases in the death receptor and mitochondrial apoptosis pathways, respectively. Both pathways eventually converge to activate caspase-3, resulting in cell apoptosis [13]. Previous reports showed that NTP could induce tumor cell apoptosis *via* different pathways, depending on the cell types, intensity of the stimulus, or the activity of other signaling pathways. For example, NTP could induce apoptosis in human melanoma cells through activation of TNF-ASK1 pathways [28]. NTP also induced death in lung cancer cells through mitochondrial-nuclear network [29]. Our results showed that NTP exposure activated caspase-9/-3 instead of caspase-8, and cleaved PARP in a dose-dependent manner. Pan-caspase inhibitors significantly blocked cell deaths induced by NTP exposure. These results provided further evidence that NTP probably induced apoptosis in HeLa cells through a mitochondria-dependent pathway.

The mitochondria pathway plays an essential role in transduction of death signals and amplification of apoptotic responses [14]. This pathway is characterized by a change in the mitochondrial membrane potential (MMP) and release of pro-apoptotic factors (cytochrome *c,* AIF, Smac etc.) from mitochondria into the cytoplasm/nucleus [30]. As such, a loss of MMP was regarded as a characteristic of mitochondria-dependent apoptosis. Consistent with these reports, our results showed that NTP increased the green fluorescence of cells, indicating a loss of MMP and mitochondrial damage [31]. In addition, the integrity of mitochondrial

membranes was regulated by proteins in the Bcl-2 family (Bcl-2 and Bax) [18]. In response to a variety of stimuli including anti-cancer drugs, Bax translocates to the mitochondria and enters the outer mitochondrial membrane, where cytochrome *c* is released. In contrast, Bcl-2 blocks cytochrome *c* efflux by binding to the outer mitochondrial membrane and forming a heterodimer with Bax resulting in neutralization of its proapoptotic effects [18,32,33]. Therefore, the balance between the levels of Bcl-2 and Bax is critical in determining the fate of cells in terms of cell survival or death. The results obtained in the present study demonstrated that NTP increased the ratio of Bax to Bcl-2, promoted Bax translocation from cytosol to mitochondria, resulting in release of cytochrome *c* from mitochondria into the cytosol, subsequently triggering apoptosis. These results further demonstrated that NTP induced apoptosis in HeLa cells through a mitochondria-dependent pathway.

ROS have important roles in a number of biological processes and have also been implied in cellular redox signaling [34]. Excessive amounts of ROS can damage cellular components such as DNA, proteins and lipids, resulting in cell death [35]. Previous studies showed that NTP generated ROS that could be the main cause of biological effects in cultured cancer cells [3,22,36,37]. Previous studies showed that NTP generated a variety of ions and free radicals, including H_2O_2, OH^-, O_2^-, O_3 and NO_3^-, which are considered as the most biologically relevant components of plasma [9]. H_2O_2 can penetrate to a depth that is sufficient to reach cells, where iron proteins could conceivably catalyze both radicals into a highly reactive OH radical that interact with cellular components [10]. Our results were consistent with other reports that NTP exposure could significantly increase intracellular H_2O_2 and ROS generation [3,36]. Meanwhile, scavenging of ROS (with NAC) could significantly suppress NTP-induced apoptosis, suggesting that ROS played a pivotal role in NTP-induced apoptosis of HeLa cells. In addition, NAC suppressed NTP-induced changes of mitochondrial membrane potential, Bax translocation and the release of cytochrome *c*. These results indicated that NTP exposure induced apoptosis in HeLa cells *via* intracellular ROS generation and mitochondria-mediated pathways. Furthermore, our findings provided a possible explanation to the previous reports that NTP could selectively or preferentially kill cancer cells with little toxicity to normal cells, or supported that the anti-cancer potential of NTP could be enhanced when combined with some chemotherapeutic agents (gemcitabine, 2-DG, cetuximab, doxorubicin and temozolomide) which could induce ROS generation [6,37,38].

In conclusion, our results showed that NTP exposure induced apoptosis in HeLa cells *via* activating ROS generation and mitochondria-mediated apoptotic signaling. Our findings provided new insights into the molecular mechanisms of NTP-induced apoptosis, and could provide information for developing NTP alone or a combination with an ROS inducer as a potential strategy for cancer therapy.

Conflicts of interest

No potential conflicts of interest were disclosed.

Acknowledgements

This work was funded by Natural Science Foundation of China (No. 81227902 and U1632145), project funded by the Priority Academic Program Development of Jiangsu Higher Education Institutions and Jiangsu Provincial Key Laboratory of Radiation Medicine and Protection, China Postdoctoral Science Foundation (No. 2016M592584), and Strategic Research Grant 7004641 from City University of Hong Kong.

References

[1] W. Kim, K.C. Woo, G.C. Kim, K.T. Kim, Nonthermal-plasma-mediated animal cell death, J. Phys. D. Appl. Phys. 44 (2011) 013001.
[2] S. Kalghatgi, C.M. Kelly, E. Cerchar, B. Torabi, O. Alekseev, A. Fridman, G. Friedman, J.A. Clifford, Effects of non-thermal plasma on mammalian cells, PLoS One 6 (2011) e16270.
[3] M. Vandamme, E. Robert, S. Lerondel, V. Sarron, D. Ries, S. Dozias, J. Sobilo, D. Gosset, C. Kieda, B. Legrain, J.M. Pouvesle, A.L. Pape, ROS implication in a new antitumor strategy based on non-thermal plasma, Int. J. Cancer 130 (2012) 2185–2194.
[4] S. Kalghatgi, G. Friedman, A. Fridman, A.M. Clyne, Endothelial cell proliferation is enhanced by low dose non-thermal plasma through fibroblast growth factor-2 release, Ann. Biomed. Eng. 38 (2010) 748–757.
[5] Z. Ke, Q. Huang, Haem-assisted dityrosine-cross-linking of fibrinogen under non-thermal plasma exposure: one important mechanism of facilitated blood coagulation, Sci. Rep. 6 (2016) 26982.
[6] L. Brulle, M. Vandamme, D. Ries, E. Martel, E. Robert, S. Lerondel, V. Trichet, S. Richard, J.M. Pouvesle, A. Le Pape, Effects of a non thermal plasma treatment alone or in combination with gemcitabine in a MIA PaCa2-luc orthotopic pancreatic carcinoma model, PLoS One 7 (2012) e52653.
[7] J. Schlegel, J. Köritzer, V. Boxhammer, Plasma in cancer treatment, Clin. Plasma Med. 1 (2013) 2–7, 2013.
[8] H. Tanaka, K. Ishikawa, M. Mizuno, S. Toyokuni, H. Kajiyama, F. Kikkawa, H.-R. Metelmann, M. Hori, State of the art in medical applications using non-thermal atmospheric pressure plasma, Rev. Mod. Plasma Phys. 1 (2017), 1: 3.
[9] H. Zhang, Z. Xu, J. Shen, X. Li, L. Ding, J. Ma, Y. Lan, W. Xia, C. Cheng, Q. Sun, Z. Zhang, P.K. Chu, Effects and mechanism of atmospheric-pressure dielectric barrier discharge cold plasma on lactate dehydrogenase (LDH) enzyme, Sci. Rep. 5 (2015) 10031.
[10] D. Xu, D. Liu, B. Wang, C. Chen, Z. Chen, D. Li, Y. Yang, H. Chen, M.G. Kong, In situ OH generation from O_2^- and H_2O_2 plays a critical role in plasma-induced cell death, PLoS One 10 (2015) e0128205.
[11] D. Ivanova, Z. Zhelev, I. Aoki, R. Bakalova, T. Higashi, Overproduction of reactive oxygen species - obligatory or not for induction of apoptosis by anticancer drugs, Chinese, J. Cancer. Re 28 (2016) 383–396.
[12] R.T. Allen, M.W. Cluck, D.K. Agrawal, Mechanisms controlling cellular suicide: role of Bcl-2 and caspases, Cell. Mol. Life. Sci. 54 (1998) 427–445.
[13] L. Duprez, E. Wirawan, T. Vanden Berghe, P. Vandenabeele, Major cell death pathways at a glance, Microbes Infect. 11 (2009) 1050–1062.
[14] S. Xiong, T. Mu, G. Wang, X. Jiang, Mitochondria-mediated apoptosis in mammals, Protein & Cell 5 (2014) 737–749.
[15] A. Aronis, J.A. Melendez, O. Golan, S. Shilo, N. Dicter, O. Tirosh, Potentiation of Fas-mediated apoptosis by attenuated production of mitochondria-derived reactive oxygen species, Cell Death Differ. 10 (2003) 335–344.
[16] Y.F. Wang, H.W. Shyu, Y.C. Chang, W.C. Tseng, Y.L. Huang, K.H. Lin, M.C. Chou, H.L. Liu, C.Y. Chen, Nickel (II)-induced cytotoxicity and apoptosis in human proximal tubule cells through a ROS- and mitochondria-mediated pathway, Toxicol. Appl. Pharm. 259 (2012) 177–186.
[17] J. Zhao, L. Zhang, J. Li, T. Wu, M. Wang, G. Xu, F. Zhang, L. Liu, J. Yang, S. Sun, A novel pyrazolone-based derivative induces apoptosis in human esophageal cells via reactive oxygen species (ROS) generation and caspase-dependent mitochondria-mediated pathway, Chem-Biol. Interact. 231 (2015) 1–9.
[18] S. Cory, J.M. Adams, The Bcl2 family: regulators of the cellular life-or-death switch, Nat. Rev. Cancer 2 (2002) 647–656.
[19] W. Li, K.N. Yu, L. Bao, J. Shen, C. Cheng, W. Han, Non-thermal plasma inhibits human cervical cancer HeLa cells invasiveness by suppressing the MAPK pathway and decreasing matrix metalloproteinase-9 expression, Sci. Rep. 6 (2016) 19720.
[20] J. Ma, H. Zhang, C. Cheng, J. Shen, L. Bao, W. Han, Contribution of hydrogen peroxide to non-thermal atmospheric pressure plasma induced A549 lung cancer cell damage, Plasma Process. Polym. 14 (7) (2017) 1600162.
[21] M. Keidar, R. Walk, A. Shashurin, P. Srinivasan, A. Sandler, S. Dasgupta, R. Ravi, R. Guerrero-Preston, B. Trink, Cold plasma selectivity and the possibility of a paradigm shift in cancer therapy, Brit. J. Cancer 105 (2011) 1295–1301.
[22] R. Sensenig, S. Kalghatgi, E. Cerchar, G. Fridman, A. Shereshevsky, B. Torabi, K.P. Arjunan, E. Podolsky, A. Fridman, G. Friedman, J. Azizkhan-Clifford, A.D. Brooks, Non-thermal plasma induces apoptosis in melanoma cells via production of intracellular reactive oxygen species, Ann. Biomed. Eng. 39 (2011) 674–687.
[23] A. Schmidt, S. Dietrich, A. Steuer, K.D. Weltmann, T. von Woedtke, K. Masur, K. Wende, Non-thermal plasma activates human keratinocytes by stimulation of antioxidant and phase II pathways, J. Biol. Chem. 290 (2015) 6731–6750.
[24] J.W. Chang, S.U. Kang, Y.S. Shin, S.J. Seo, Y.S. Kim, S.S. Yang, J.S. Lee, E. Moon, K. Lee, C.H. Kim, Combination of NTP with cetuximab inhibited invasion/migration of cetuximab-resistant OSCC cells: involvement of NF-kappaB signaling, Sci. Rep. 5 (2015) 18208.
[25] G.P. Sykiotis, A.G. Papavassiliou, Apoptosis: the suicide solution in cancer treatment and chemoprevention, Expert. Opin. Inv. Drugs 15 (2006) 575–577.
[26] S. Kasibhatla, B. Tseng, Why target apoptosis in cancer treatment? Mol. Cancer Ther. 2 (2003) 573–580.
[27] R. Gerl, D.L. Vaux, Apoptosis in the development and treatment of cancer, Carcinogenesis 26 (2005) 263–270.
[28] M. Ishaq, S. Kumar, H. Varinli, Z.J. Han, A.E. Rider, M.D. Evans, A.B. Murphy,

K. Ostrikov, Atmospheric gas plasma-induced ROS production activates TNF-ASK1 pathway for the induction of melanoma cancer cell apoptosis, Mol. Biol. Cell 25 (2014) 1523–1531.
[29] T. Adachi, H. Tanaka, S. Nonomura, H. Hara, S. Kondo, M. Hori, Plasma-activated medium induces A549 cell injury via a spiral apoptotic cascade involving the mitochondrial-nuclear network, Free Radic. Bio. Med 79 (2015) 28–44.
[30] Y. Shi, A structural view of mitochondria-mediated apoptosis, Nat. Struct. Biol. 8 (2001) 394–401.
[31] K. Panngom, K.Y. Baik, M.K. Nam, J.H. Han, H. Rhim, E.H. Choi, Preferential killing of human lung cancer cell lines with mitochondrial dysfunction by nonthermal dielectric barrier discharge plasma, Cell Death Dis. 4 (2013) e642.
[32] C.Y. Cheng, C.C. Su, Tanshinone IIA may inhibit the growth of small cell lung cancer H146 cells by up-regulating the Bax/Bcl-2 ratio and decreasing mitochondrial membrane potential, Mol. Med. Rep. 3 (4) (2010) 645–650.
[33] X. Yan, Z. Jiang, L. Bi, Y. Yang, W. Chen, Salvianolic acid A attenuates TNF-alpha- and D-GalN-induced ER stress-mediated and mitochondrial-dependent apoptosis by modulating Bax/Bcl-2 ratio and calcium release in hepatocyte LO2 cells, N-S.Arch. Pharm. 388 (2015) 817–830.
[34] J. Wang, J. Yi, Cancer cell killing via ROS: to increase or decrease, that is the question, Cancer Biol. Ther. 7 (2008) 1875–1884.
[35] X. Feng, W. Yu, F. Zhou, J. Chen, P. Shen, A novel small molecule compound diaporine inhibits breast cancer cell proliferation via promoting ROS generation, Biom. Pharmacother. 83 (2016) 1038–1047.
[36] S.U. Kang, J.H. Cho, J.W. Chang, Y.S. Shin, K.I. Kim, J.K. Park, S.S. Yang, J.S. Lee, E. Moon, K. Lee, C.H. Kim, Nonthermal plasma induces head and neck cancer cell death: the potential involvement of mitogen-activated protein kinase-dependent mitochondrial reactive oxygen species, Cell Death Dis. 5 (2014) e1056.
[37] N. Kaushik, N. Uddin, G.B. Sim, Y.J. Hong, K.Y. Baik, C.H. Kim, S.J. Lee, N.K. Kaushik, E.H. Choi, Responses of solid tumor cells in DMEM to reactive oxygen species generated by non-thermal plasma and chemically induced ROS systems, Sci. Rep. 5 (2015) 8587.
[38] N. Kaushik, S.J. Lee, T.G. Choi, K.Y. Baik, H.S. Uhm, C.H. Kim, N.K. Kaushik, E.H. Choi, Non-thermal plasma with 2-deoxy-D-glucose synergistically induces cell death by targeting glycolysis in blood cancer cells, Sci. Rep. 5 (2015) 8726.